

# IDENTIFICATION OF THE AEROACOUSTIC RESPONSE OF DUCTED LOW MACH NUMBER FLOWS

Paula Martínez-Lera<sup>\*1</sup>, Christophe Schram<sup>2</sup>, Stephan Föller<sup>3</sup>, Roland Kaess<sup>3</sup>,  
Wolfgang Polifke<sup>3</sup>

<sup>1</sup> Simulation Division, LMS International,  
Interleuvenlaan 68, 3001 Leuven, Belgium

<sup>2</sup> EA and AR Departments, von Karman Institute for Fluid Dynamics  
Chaussée de Waterloo 72, 1640 Rhode-St-Genèse, Belgium

<sup>3</sup> Lehrstuhl für Thermodynamik, Technische Universität München  
Boltzmannstr. 15, D-85747 Garching, Germany

\* Corresponding author: paula.martinez@lmsintl.com

In some elements of piping systems, such as T-joints, shear layers can provide a feedback mechanism for acoustic resonances. The mechanism works as follows: Acoustic waves produce vortical disturbances in an unstable shear layer, which are amplified and convected downstream. During their convection, these flow disturbances interact with the acoustic field either constructively, thus resulting in a net sound production, or destructively, thus resulting in a net sound absorption. Modeling the sound production by the shear layer as a response to an acoustic excitation becomes necessary to predict resonance phenomena such as whistling.

The sound production at an element of a piping system as a reaction to an acoustic field can be characterized by a transfer matrix that relates input and output acoustic variables. If the amplitude of the acoustic velocity is small with respect to the main speed of the flow, then the transfer matrix provides a linear relationship between the acoustic variables. If the acoustic amplitude increases, the shear layer starts to saturate as a result of vortex roll-up. In this case, the response of the flow becomes nonlinear, with the elements of the transfer matrix depending also on the acoustic variables. While the linear regime of the shear layer characterizes the onset of resonances, nonlinearities are key to predict the limit-cycle amplitude of the oscillations.

In this work, the sound production in an acoustically compact T-joint as a response of the shear layer to an acoustic field has been modeled with numerical techniques. The deviation from the linear regime due to nonlinearities in the flow as a consequence of vortex roll-up has been investigated.

The numerical study is based on incompressible two-dimensional CFD simulations, excited with external velocity perturbations. The sound production is obtained using an acoustic analogy based on vortex sound theory [4]. The proposed methodology treats the T-joint element as a black-box, and can therefore be applied to investigate the aeroacoustic response of ducted flows with arbitrary geometries.

In the linear regime, a single flow computation of the T-joint excited with a broadband signal provides information about all acoustic modes and for the whole frequency range of interest, by applying linear identification techniques, which are here based on the Wiener-Hopf equation [1, 9]. However, in the nonlinear regime, a separate computation is needed for each frequency and acoustic mode.

The results illustrate the transition from the linear to the nonlinear regime as the acoustic amplitude increases and the shear layer starts to roll up in vortices. The onset of nonlinear-

ities depends strongly on flow parameters such as the boundary layer thickness. Nevertheless, some general trends are also observed, that are similar for every flow case investigated and in good agreement with experimental results available in the literature. Moreover, the results illustrate that, while the linear and transition regimes depend strongly on the flow features, the source models in the full nonlinear regime are much less sensitive to the details of the flow model, thus better representing a generic T-joint. The obtained numerical models are compared to experimental results available in the literature, notably with those provided by Graf and Ziada [2, 3].

The main results that will be shown in this presentation can be found in References [5, 6]. Some improvements on the methodology have been recently proposed by Nakiboglu and Hirschberg [7, 8].

## References

- [1] S. Föllner, R. Kaess, and W. Polifke. Reconstruction of acoustic transfer matrices from large-eddy-simulation of complex turbulent flows. In *AIAA*, number Paper 2008-3046, 2008.
- [2] H. R. Graf and S. Ziada. Flow induced acoustic resonance in closed side branches: an experimental determination of the excitation source. In *AMD-Vol. 151/PVP-Vol.247, Symposium on Flow-Induced Vibration and Noise*, volume 7, 1992.
- [3] H. R. Graf and S. Ziada. Excitation source of a side-branch shear layer. *J. Sound Vib.*, 329:2825–2842, 2010.
- [4] M. S. Howe. Contributions to the theory of aerodynamic sound, with application to excess jet noise and the theory of the flute. *J. Fluid Mech.*, 71(4):625–673, 1975.
- [5] P. Martínez-Lera, S. Föllner, R. Kaess, B. Karthik, C. Schram, and W. Polifke. Low-order modeling of a side branch at low Mach numbers. In *15th AIAA/CEAS Aeroacoustics Conference, Miami, US*, number AIAA 2009-3263, 2009.
- [6] P. Martínez-Lera, C. Schram, S. Föllner, R. Kaess, and W. Polifke. Identification of the aeroacoustic response of a low Mach number flow through a T-joint. *J. Acoust. Soc. Am.*, 126(2):582–586, 2009.
- [7] G. Nakiboglu and A. Hirschberg. A numerical study of the aeroacoustic interaction of a cavity with a confined flow: Effect of edge geometry in corrugated pipes. In *Proceedings of ASME, FEDSM2010-ICNMM2010*, number 30300, 2010.
- [8] G. Nakiboglu and A. Hirschberg. A numerical study on the effect of confinement ratio in whistling corrugated pipes. In *ICSV17, 17th International Congress on Sound and Vibration*, 2010.
- [9] W. Polifke, A. Poncet, C. O. Paschereit, and K. Döbbling. Reconstruction of acoustic transfer matrices by stationary Computational Fluid Dynamics. *J. Sound Vib.*, 245:483–510, 2001.

# Low-order modeling of a side branch at low Mach numbers

P. Martínez-Lera<sup>\*</sup>, B. Karthik<sup>†</sup>, C. Schram<sup>‡</sup>

*LMS International, 3001 Leuven, Belgium*

S. Föller<sup>§</sup>, R. Kaess<sup>¶</sup>, W. Polifke<sup>||</sup>

*Technische Universität München, D-85747 Garching, Germany*

Network models are used in this work to study the behavior of a piping system with a side branch. Linear and nonlinear models of the sound production in the shear layer of a T-joint, which are obtained numerically, are integrated in the network model. A three-dimensional finite element computation is carried out to characterize the acoustic impedance of an additional element of the network. This combination of numerical techniques provides an approach to study the stability and limit-cycle amplitude of a piping system.

## I. Introduction

In piping systems, the shear layer in T-joints can provide a feedback mechanism for acoustic resonances. For this reason, the sound production in a T-joint has been object of both experimental and numerical studies in the past.<sup>1,2,3,4,5,6</sup> In this work, the flow-generated sound in a pipe with a closed side branch is investigated through numerical techniques. The objective is to integrate in a network model a model of the sound production in a T-joint, in order to study its interaction with other elements of a piping system.

Network models represent a useful tool to study the stability of piping systems. However, some elements of the network model may be difficult to characterize analytically, either because of involving aeroacoustic sources, as in the case of the T-joint, or simply because of a complex geometry. Models for such elements may be obtained numerically. The source model for the T-joint can be obtained through a combination of flow computations and acoustic analogies.<sup>3,7</sup> The acoustic impedance of elements of a piping system with a complex geometry can be calculated with numerical techniques such as finite element or boundary element methods.

In the present work, such combination of three- or two-dimensional numerical computations and network models is applied to study the stability and limit-cycle amplitude of a piping system that includes a T-joint. The outline of the paper is the following. In Section II, the configuration of the considered T-joint is discussed, and source models for the linear and the nonlinear regimes of the shear layer are obtained. In Section III, a model for an area expansion in a duct is obtained through a finite element method. In Section IV, all the elements (T-joint, area expansion) of a considered piping system are integrated in a network model in order to study the stability and limit-cycle amplitude. Section V contains a final discussion about the advantages and limitations of the methods studied.

---

<sup>\*</sup>PhD Candidate, Simulation Division, Interleuvenlaan 68.

<sup>†</sup>Dr, Senior Research Engineer, Simulation Division, Interleuvenlaan 68.

<sup>‡</sup>Dr, RTD Project Manager, Simulation Division, Interleuvenlaan 68, AIAA Member.

<sup>§</sup>PhD Candidate, Lehrstuhl für Thermodynamik, Boltzmannstr. 15.

<sup>¶</sup>PhD Candidate, Lehrstuhl für Thermodynamik, Boltzmannstr. 15.

<sup>||</sup>Professor, Lehrstuhl für Thermodynamik, Boltzmannstr. 15.

## II. Shear layer source models

### A. Description of the problem

In a T-joint, the shear layer can interact with acoustic waves present in the ducts, either absorbing or producing additional sound. The feedback mechanism is the following. The acoustic field produces vortical disturbances in the unstable shear layer, which are amplified and convected downstream. During their convection in the shear layer, these flow disturbances interact with the acoustic field either constructively, thus resulting in a net sound production, or destructively, thus resulting in a net sound absorption. The elements involved in this feedback mechanism are illustrated in Figure 1.

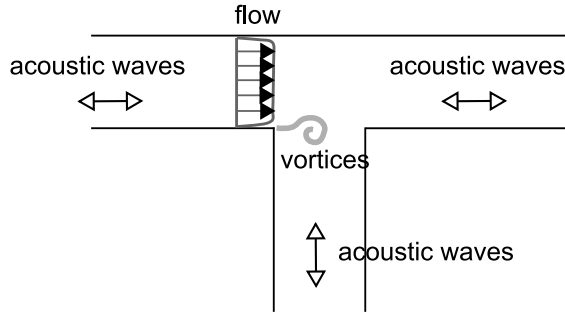


Figure 1. Elements involved in the flow-acoustic feedback mechanism in a T-joint.

The response of the shear layer depends strongly on the amplitude of the acoustic field. For low acoustic amplitudes, the shear layer gives a response that is linear with the acoustic excitation. Moderate and high acoustic amplitudes, by contrast, lead to saturation of the growing instabilities in the shear layer, and therefore the response becomes nonlinear. Flow parameters, such as the velocity profile at the upstream edge, and geometry characteristics influence also significantly the response of the shear layer; nevertheless, this will not be tackled in this paper, which is restricted to a particular T-joint configuration and fixed flow parameters.

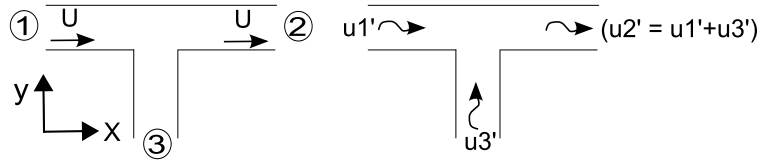


Figure 2. T-joint: main flow and acoustic flow.

The considered configuration is illustrated in Figure 2. The main duct and the side branch have the same diameter  $D$ . The main flow enters through inlet 1 and exits through outlet 2. The Reynolds number based on the mean flow velocity  $U$  and on  $D$  is  $Re = 1,000$ . The flow is considered incompressible, with uniform density  $\rho_0$ . The boundary layer at the upstream edge of the joint is laminar and has a momentum thickness  $\theta = 0.026D$  defined as

$$\theta = \int_{y_w}^{y_c} \frac{u(y)}{U_c} \left(1 - \frac{u(y)}{U_c}\right) dy, \quad (1)$$

where  $u(y)$  is the  $x$ -velocity profile,  $U_c$  is the  $x$ -velocity at the centerline of the duct, and  $y_w$  and  $y_c$  are, respectively, the  $y$ -coordinates of the lower wall and of the centerline of the duct.

Different authors have proposed source models for similar configurations, obtaining these models either analytically,<sup>8</sup> experimentally<sup>2</sup> or numerically.<sup>3</sup> In the present work, the numerical approach proposed by Martínez-Lera *et al.*<sup>7</sup> is applied to obtain the linear response of the shear layer. This approach combines incompressible CFD simulations, an acoustic analogy based on vortex sound theory and system identification techniques, and

is suitable for flows with a low Mach number and through acoustically compact T-joints. The method is briefly discussed in the following section.

## B. Modeling the linear regime of the shear layer

The aim is to find a transfer matrix that relates the acoustic velocity perturbations ( $u'_1$  and  $u'_3$  as defined in Figure 2) to the source pressure jumps due to the shear layer,  $(\Delta p_s)_{12}$  between the inlet duct and the outlet duct, and  $(\Delta p_s)_{32}$  between the side branch and the outlet duct. The transfer matrix  $\mathbf{A}$  is defined so that

$$\begin{pmatrix} (\Delta p_s)_{12} \\ (\Delta p_s)_{32} \end{pmatrix} = \rho_0 U \mathbf{A}(Sr) \cdot \begin{pmatrix} u'_1 \\ u'_3 \end{pmatrix} = \rho_0 U \begin{pmatrix} a_{11}(Sr) & a_{12}(Sr) \\ a_{21}(Sr) & a_{22}(Sr) \end{pmatrix} \cdot \begin{pmatrix} u'_1 \\ u'_3 \end{pmatrix}, \quad (2)$$

where  $Sr = Df/U$  is the Strouhal number related to the acoustic frequency  $f$ . Matrix  $\mathbf{A}$  is obtained in three steps:<sup>7</sup>

1. **Incompressible CFD simulation:** A two-dimensional incompressible simulation is carried out using a laminar second-order implicit solver of a commercial software (Fluent 6.3). In this simulation, two uncorrelated time-dependent velocity perturbations  $u'_1$  and  $u'_3$  are added at the main inlet 1 and side-branch inlet 3. These signals have a broadband frequency content and a low amplitude ( $< 0.001U$ ), so that the shear layer response is linear. The area-averaged total pressure  $P = p + \rho_0 u^2/2$  at several sections of the duct is stored at each time step during the CFD simulation. The response of the flow to the excitations is measured in terms of the total pressure jumps  $\Delta P_{12}$  and  $\Delta P_{32}$  between the inlet duct and the outlet duct, and between the side branch and the outlet duct, respectively.
2. **Source processing:** The pressure jumps due to the sound production of the shear layer represent only a fraction of the total pressure jumps measured during the CFD simulation. Therefore, these must be post-processed in order to obtain the sources of sound. This is done by applying an acoustic analogy based on vortex sound theory. For an incompressible fluid and neglecting viscous effects, the momentum equation yields

$$\nabla P = -\rho_0 \frac{\partial \mathbf{u}}{\partial t} - \rho_0 (\boldsymbol{\omega} \times \mathbf{u}), \quad (3)$$

where  $\boldsymbol{\omega}$  represents vorticity. The second term on the right-hand side of Equation (3) is related to the acoustic power according to Howe's energy corollary,<sup>9</sup> being thus related to the source pressure jump. By contrast, the first term is related to a potential solution of the flow. This term produces a pressure jump  $\Delta p_{pot}$  that is not related to the sound production

$$\Delta p_{pot} = -\rho_0 \frac{\partial u_l}{\partial t} \int_L dl, \quad (4)$$

and that, for an incompressible flow, is proportional to the distance  $L$  traveled by the flow along the longitudinal coordinate  $l$  of the duct. It can be identified using Equation 4 and subtracted from the total pressure jump, in order to obtain the source pressure jump.

3. **Matrix identification:** Matrix  $\mathbf{A}$ , which relates the source pressure jumps to the acoustic velocities  $u'_1$  and  $u'_3$  according to Equation (2), is computed by applying a method based on the Wiener-Hopf equation, that has been applied in the past to the reconstruction of acoustic transfer matrices.<sup>10,11</sup>

Figure 3 provides results of the matrix coefficients in the linear regime, together with results corresponding to the nonlinear regime, which are discussed in the following section.

## C. Modeling the nonlinear regime of the shear layer

If the acoustic amplitude increases, the shear layer starts to saturate as a result of vortex roll-up. This introduces nonlinearities in the acoustic behavior of the shear layer. In this case, the transfer matrix does not only depend on the frequency, but also on the amplitude of the acoustic field:  $(\mathbf{A})_{\text{nonlinear}} = \mathbf{A}(Sr, u')$ . As the superposition principle is not satisfied anymore, the matrix cannot be obtained from a single CFD simulation, as was the case for the linear regime. Separate computations need to be run for each frequency, acoustic

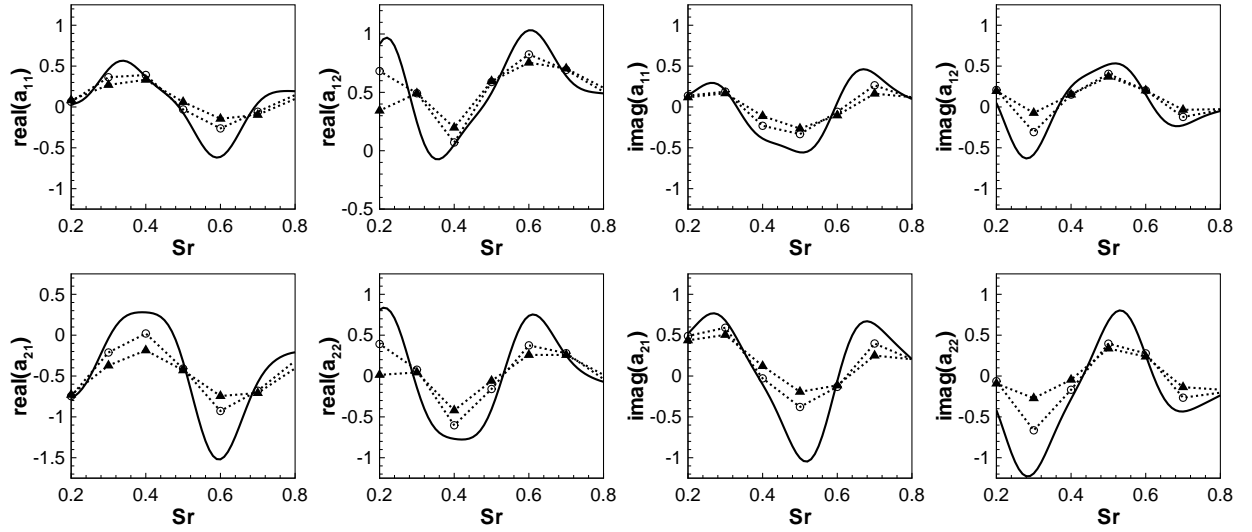


Figure 3. Source model for a T-joint: Matrix A coefficients. Linear regime (solid line),  $u' = 0.1U$  (circles),  $u' = 0.2U$  (triangles).

amplitude and direction of the acoustic flow, as done by Hofmans<sup>3</sup> with a vortex blob method. Simulations are carried out with single excitations  $u'(t) = |u'| \sin(2\pi ft)$  either at the inlet or at the side branch, with the following parameters:

- Strouhal numbers  $Sr = 0.2, 0.3, 0.4, 0.5, 0.6, 0.7$  and  $0.8$ .
- Acoustic flow directions from inlet 1 to outlet 2 ( $u' = u'_1$ , for coefficients  $a_{11}$  and  $a_{21}$ ) and acoustic flow directions from side branch 3 to outlet 2 ( $u' = u'_3$ , for coefficients  $a_{12}$  and  $a_{22}$ ).
- Acoustic amplitudes  $|u'| = 0.05U, 0.1U$  and  $0.2U$ .

The CFD results are post-processed to extract the sources following the same technique as for the linear regime, based on vortex sound theory. As in the nonlinear case a single excitation with only one frequency is applied, the coefficients of the matrix are obtained as the ratio of the Fourier coefficients of the source pressure jump and the acoustic velocity for the excitation frequency, without having to apply any additional system identification technique.

Figure 3 shows the dependency of the matrix coefficients on the acoustic amplitude and Strouhal number. It must be stressed that, although in the linear regime the coefficients of matrix A describe the response of the shear layer to all possible acoustic configurations, as they are a linearly dependent on the others, in the nonlinear regime however the matrix coefficients only give information about the two computed acoustic configurations:

1.  $u'_1 = u'$  and  $u'_3 = 0$ , and
2.  $u'_1 = 0$  and  $u'_3 = u'$ .

For example, for a side branch with an acoustic excitation traveling between the main inlet 1 and the side branch 3 ( $u'_1 = u'$  and  $u'_3 = -u'$ ), matrix A would give the response of the system in the linear regime, as this mode is a linear combination of the two mentioned modes. However, additional computations would be necessary to characterize the behavior for this mode in the nonlinear regime.

### III. FEM computation of acoustic elements

Three-dimensional numerical simulations can be used to characterize the acoustic behavior of elements of a network that have a complex geometry or, simply, for which analytical models are not readily available. In this section, a 1D model of the acoustic behavior of an area expansion in a duct is obtained by solving the Helmholtz equation in the interior of the duct through Finite Element Method (FEM). For this purpose, the commercial software Virtual.Lab 8A is used.

Figure 4 shows the considered geometry and mesh. The diameters of the ducts are  $D_{\text{in}} = 0.15 \text{ m}$  and  $D_{\text{out}} = 1 \text{ m}$ . The mesh contains 5,520 hexahedral elements. An acoustic velocity  $u'$  is imposed as a boundary condition at the end with the smaller section, which is considered the inlet. An acoustic impedance  $Z = \rho_0 c_0$  is prescribed at the outlet, with  $\rho_0 = 1.225 \text{ kg/m}^3$  and  $c_0 = 340 \text{ m/s}$  being the speed of sound.

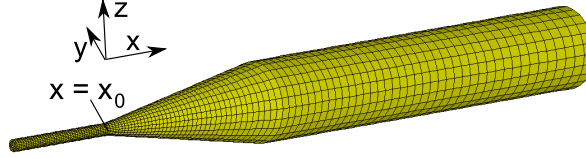


Figure 4. FEM model of an area expansion element.

The 1D model is characterized through the reflection coefficient  $R$  at the beginning of the expansion ( $x = x_0$ ), defined as

$$R(x) = \frac{p'(x) - \rho_0 c_0 u'(x)}{p'(x) + \rho_0 c_0 u'(x)}. \quad (5)$$

where  $p'(x)$  and  $u'(x)$  are obtained by averaging the acoustic pressure and velocity over the considered section.  $R$  is however not directly measured at  $x = x_0$ , as in the region of the expansion the propagation is not like the one of plane waves, and the calculation of  $R$  becomes inaccurate. Instead, the reflection coefficient is measured at  $x = x_0 - D_{\text{in}}$ , and the reflection coefficient at  $x = x_0$  is determined as

$$R(x = x_0) = R(x = x_0 - D_{\text{in}}) e^{2i \frac{\omega}{c_0} D_{\text{in}}}, \quad (6)$$

where  $\omega$  is the angular frequency.

Figure 5 shows the reflection coefficient as a function of frequency. It can be observed that for low frequencies, the reflection coefficient tends to the one of a sudden area expansion  $R_0$ :

$$R_0 = \frac{1 - D_{\text{out}}^2/D_{\text{in}}^2}{1 + D_{\text{out}}^2/D_{\text{in}}^2} = -0.956. \quad (7)$$

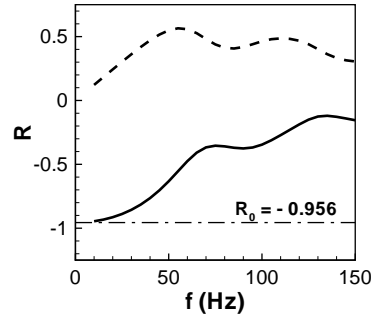


Figure 5. Reflection coefficient: real part (solid) and imaginary part (dashed).

## IV. System network model

### A. Description of a generic model

The interaction of a T-joint with other elements of a piping system is studied through network models.<sup>12</sup> An example of a system is presented in Figure 6.

The equations are written in terms of the Riemann invariants  $f$  and  $g$ , defined as

$$f = \frac{1}{2} \left( \frac{p'}{\rho_0 c_0} + u' \right) \quad (8)$$

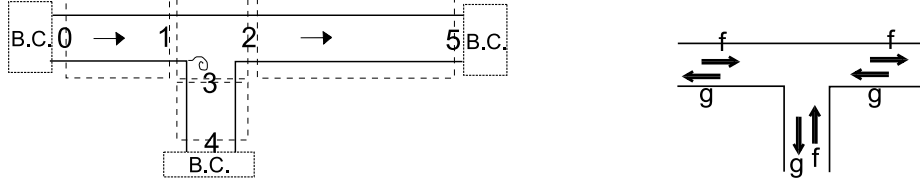


Figure 6. Duct with a side branch. The elements that this system comprises are: straight ducts between 0 and 1, between 2 and 5 and between 3 and 4; a T-joint joining 1, 2 and 3, and three boundary conditions (BC) at 0, 4 and 5.

and

$$g = \frac{1}{2} \left( \frac{p'}{\rho_0 c_0} - u' \right). \quad (9)$$

The convention for the direction of the Riemann invariants can be seen in Figure 6.

The acoustic wavenumber is denoted as  $k_0 = 2\pi f/c_0$ . When convective effects are included, and a model is used to characterize viscous losses,<sup>13</sup> two different wavenumbers  $k^+$  and  $k^-$  are defined:

$$k^\pm = \frac{k_0}{1 \pm M} \left( 1 + (1 - i) \frac{\delta_v}{D} \left( 1 + \frac{\gamma - 1}{\sqrt{Pr}} \right) \right), \quad (10)$$

where  $M$  is the Mach number  $M = U/c_0$ ,  $Pr = 0.71$  is the Prandtl number,  $\gamma = 1.4$  is the adiabatic index of the gas, and  $\delta_v$  is the acoustic boundary layer thickness defined as

$$\delta_v = \sqrt{\frac{\nu}{\pi f}}. \quad (11)$$

The equations that characterize each of the type of elements included in the network model are the following.

- Straight duct of length  $L$  with an inlet port ‘in’ and an outlet port ‘out’:

$$f_{\text{out}} = f_{\text{in}} e^{-ik^+L}$$

and

$$g_{\text{in}} = g_{\text{out}} e^{-ik^-L}$$

- Boundary conditions, such as an open end ( $f + g = 0$ ), closed end ( $f - g = 0$ ), or, more generally, boundary conditions defined through a reflection coefficient  $R$ , such as  $-Rf + g = 0$ .
- T-joint with three ports ‘in’, ‘out’ and ‘sb’, where the main (aerodynamic) flow enters through the inlet ‘in’ and exits through the outlet ‘out’. By convention, the third port ‘sb’, corresponding to the side branch, is treated as an additional inlet. The considered model for the T-junction includes a mass conservation equation

$$f_{\text{in}} - g_{\text{in}} + f_{\text{sb}} - g_{\text{sb}} - f_{\text{out}} + g_{\text{out}} = 0, \quad (12)$$

and two additional equations that are based on the lumped 1D model obtained in Section II:

$$(p'_{\text{in}} - p'_{\text{out}}) = \rho_0 U (a_{11} u'_{\text{in}} + a_{12} u'_{\text{sb}}) \quad (13)$$

and

$$(p'_{\text{sb}} - p'_{\text{out}}) = \rho_0 U (a_{21} u'_{\text{in}} + a_{22} u'_{\text{sb}}). \quad (14)$$

Expressing these equations as function of the Riemann invariants, the two additional equations for this model are obtained:

$$(1 - Ma_{11})f_{\text{in}} + (1 + Ma_{11})g_{\text{in}} - f_{\text{out}} - g_{\text{out}} - Ma_{12}f_{\text{sb}} + Ma_{12}g_{\text{sb}} = 0 \quad (15)$$

and

$$-Ma_{21}f_{\text{in}} + Ma_{21}g_{\text{in}} - f_{\text{out}} - g_{\text{out}} + (1 - Ma_{22})f_{\text{sb}} + (1 + Ma_{22})g_{\text{sb}} = 0. \quad (16)$$

It may be noted that if the matrix coefficients were zero, this condition would be reduced to prescribing a uniform pressure in the T-joint.



With these equations for the elements shown in Figure 6, we obtain a system of 12 equations with 12 unknowns: six equations corresponding to three straight ducts, three equations for the T-joint and three boundary conditions. The stability of the system can be studied by computing the eigenfrequencies of the system. Eigenfrequencies with negative imaginary parts will involve a growth of the instability. The growth rate is calculated as<sup>12</sup>

$$\Gamma = e^{-2\pi \Im(\omega_0)/\Re(\omega_0)} - 1, \quad (17)$$

where  $\omega_0$  represents the eigenfrequency.

## B. Stability study through a network model

Figure 7 shows a scheme of the two network models that are considered as illustrative examples. They both consist of three pipes of diameter  $D = 0.15\text{ m}$  joined by a T-joint. The pipe (element 1) corresponding to the main inlet of the T-joint (element 5) ends in what can be modeled as an open end (element 0) and has a length  $L_1 = 1.25\text{ m}$ . The pipe (element 2) corresponding to the outlet of the T-joint ends in an area expansion (element 6) of reflection coefficient  $R$ , as defined by Equation (5), and has the same length  $L_2 = 1.25\text{ m}$ . The mean flow velocity in these two pipes is  $U = 34\text{ m/s}$ . The side branch (element 3) has a length  $L_3 = 0.30\text{ m}$ , and leads to a closed end (element 4).

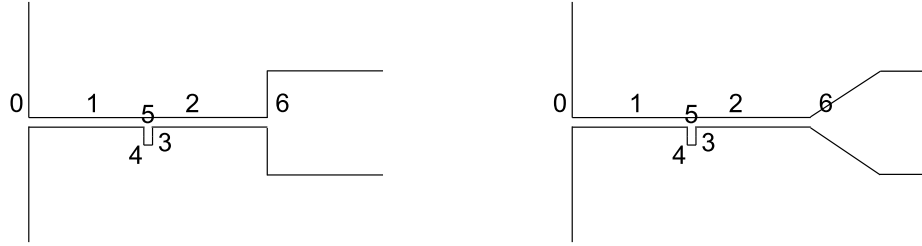


Figure 7. Studied network models: a) ending in a sudden area expansion (left); b) ending in a gentler area expansion (right).

The stability study shows that the frequency most prone to instability corresponds to approximately  $f \simeq c_0/(L_1 + L_2) = 136\text{ Hz}$ . This corresponds to an acoustic flow along the main pipe ( $u' = u'_1 \simeq u'_2$  and  $u'_3 \simeq 0$ ), and to a Strouhal number of  $Sr \simeq 0.6$ . For this Strouhal number, the real part of coefficient  $a_{11}$  of the source matrix presents a minimum. This corresponds to a maximum in the generated acoustic power  $W$ , which is under these conditions

$$W = (p'_2 - p'_1)u' \simeq -a_{11}|u'|^2. \quad (18)$$

Figure 8 shows the growth rate of the instability as a function of the reflection coefficient  $R$  of element 6 of the network. For high values of  $|R|$ , the growth rate is  $\Gamma > 0$ , and therefore the system is unstable. If the expansion is sudden (left network model in Figure 7), with a diameter ratio of  $D_{\text{in}}/D_{\text{out}} = 0.15$ , the reflection coefficient according to Equation (7) is  $R = -0.956$ . This value leads to an unstable system where the growth rate is around 2%.

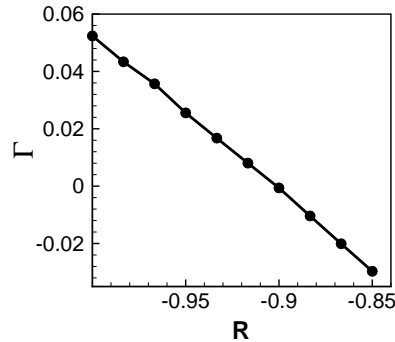


Figure 8. Growth rate for the network model vs reflection coefficient  $R$ .

The network model can be used to design a stable system, and to study what the effect of a conical expansion would be on the stability. Instead of a sudden expansion, the conical expansion described in Section III can be included in the system. This element is modeled through the frequency-dependent reflection coefficient  $R$  computed in section III through a finite element model. With this new boundary condition, the growth ratio for the eigenfrequency becomes  $\Gamma \simeq -33\% < 0$ , indicating that the system is stable.

### C. Computation of the limit-cycle amplitude

For the simple network model under consideration, the conditions for the onset of a resonance around a frequency of  $f \simeq 136\text{Hz}$  have been illustrated. This resonance corresponds also to one of the acoustic modes for which the nonlinear model discussed in Section II.C is valid. Therefore, the nonlinear model can be used to predict the limit-cycle amplitude of the system (provided that it is within the studied range of acoustic amplitudes).

The range of coefficient  $R$  that involves a positive growth rate in the linear regime according to Figure 8 is considered. For each value of  $R$ , the resulting limit-cycle acoustic amplitude is the one that makes the growth rate  $\Gamma = 0$  and, to obtain it, computations with increasing values of  $u'$  are carried out, until  $\Gamma = 0$ . As discussed in section II, higher values of  $u'$  make the source transfer matrix  $A$  dependent on the value of  $u'$ . The value of the coefficients of the matrix is obtained by interpolating from a lookup table that contains the information generated by the computations presented in section II.C. The interpolation is linear with respect to  $Sr$  and with respect to  $\log(u')$ . Figure 9 shows the limit-cycle amplitude computed like this.

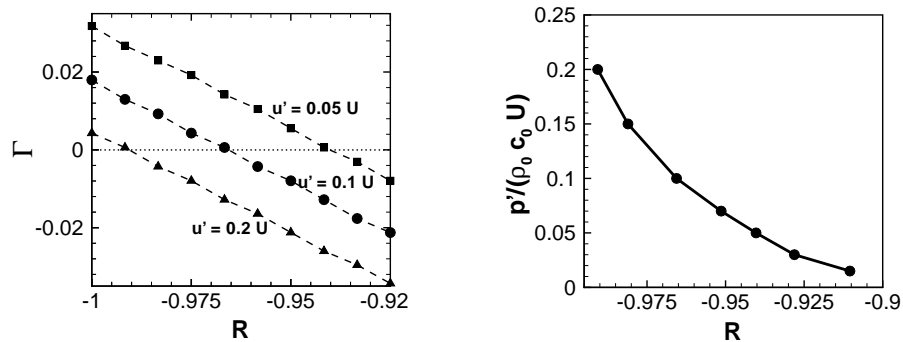


Figure 9. Growth rate vs reflection coefficient for different values of  $u'/U$  (left) and dimensionless limit-cycle acoustic amplitude  $p'/(ρ₀c₀U) = u'/U$  vs reflection coefficient  $R$  (right).

## V. Discussion

In this work, the interaction of a T-joint with other elements of a piping system has been studied by integrating a source model in a network model. The source model has been obtained numerically through CFD simulations, from which the sources are calculated by applying an acoustic analogy based on vortex sound theory.

These source models are by no means universal, as they depend strongly on the flow and geometry characteristics, such as the boundary layer thickness at the upstream edge of the joint, the curvature radius of the edges or the ratio of main duct and side-branch diameters. For this reason, it represents an advantage to be able to obtain the source models through numerical simulations, in which the flow and geometry conditions can be easily changed.

The approach has some limitations. The stability and limit-cycle amplitude predictions are only as good as the source models. The method is restricted to low Mach number flows and acoustically compact configurations. Moreover, the nonlinear regime modeling requires many computations, becoming computationally expensive. Nevertheless, the linear regime of the shear layer in a T-joint can be efficiently characterized by a single CFD computation.

Other elements of the network can be modeled through three-dimensional finite element computations. This has been illustrated for the case of an area expansion, but can be

applied in general to elements with complex geometry or for which no analytical model is available. This combination of three-dimensional numerical computations and modular one-dimensional network models provides a useful engineering tool to help in the design and analysis of piping systems.

The presented results for a particular network model serve the purpose of illustrating the methodology and its capabilities, although their accuracy is limited by the accuracy of the source model. In particular, the fact that this is obtained through two-dimensional CFD computations may have a significant impact on the results.

## Acknowledgments

The authors gratefully acknowledge the support of the European Commission for this work, performed within the FP6 Marie Curie RTN project AETHER (contract nr MRTN-CT-2006-035713). Financial support by Deutsche Forschungsgemeinschaft for Roland Kaess (Po 710/3) and Stephan Föller (Po 710/5) is also gratefully acknowledged.

## References

- <sup>1</sup>J.C. Bruggeman, *Aeroacoustic sources in internal flows*, PhD Thesis, Eindhoven University of Technology, P.O Box 90159, 5600 RM Eindhoven, The Netherlands, 1987.
- <sup>2</sup>H.R. Graf, S. Ziada, "Flow induced acoustic resonance in closed side branches: an experimental determination of the excitation source", AMD-Vol. 151/PVP-Vol.247, *Symposium on Flow-Induced Vibration and Noise*, Volume 7, ASME 1992.
- <sup>3</sup>G.C.J. Hofmans, *Vortex Sound in Confined Flows*, PhD Thesis, Eindhoven University of Technology, P.O Box 90159, 5600 RM Eindhoven, The Netherlands, 1998.
- <sup>4</sup>S. Ziada and S. Shine, "Strouhal numbers of flow-excited acoustic resonance of closed side branches", *J. Fluid Struct.* 13, 127-142, 1999.
- <sup>5</sup>M.C.A.M Peters and E. van Bokhorst, "Flow-induced pulsations in pipe systems with closed branches, impact of flow direction", 7th International Conference on Flow-Induced Vibration, Lucerne, Switzerland, 19-21 June, 2000.
- <sup>6</sup>S. Dequand, S.J. Hulshoff, A. Hirschberg, "Self-sustained oscillations in a closed side branch system", *J. Sound Vib.* 265, 359-386, 2003.
- <sup>7</sup>P. Martínez-Lera, S. Föller, R. Kaess, C. Schram, W. Polifke, "Identification of the aeroacoustic response of a low Mach number flow through a T-joint", Letter to the Editor, conditionally accepted for publication in *J. Acoust. Soc. Am.*, 2009.
- <sup>8</sup>M.S. Howe, *Acoustics of fluid-structure interactions*, Cambridge Monographs in Mechanics, Cambridge University Press, 1998.
- <sup>9</sup>M.S. Howe, *Theory of Vortex Sound*, Cambridge Texts in Applied Mathematics, 2003.
- <sup>10</sup>W. Polifke, A. Poncet, C. O. Paschereit, K. Döbbeling, "Reconstruction of Acoustic Transfer Matrices by Instationary Computational Fluid Dynamics", *J. Sound Vib.* 245, 483-510, 2001.
- <sup>11</sup>S. Föller, R. Kaess, W. Polifke, "Reconstruction of Acoustic Transfer Matrices from Large-Eddy-Simulations of Complex Turbulent Flows", AIAA Paper 2008-3046, 2008.
- <sup>12</sup>J. Kopitz, W. Polifke, "CFD-based application of the Nyquist criterion to thermo-acoustic instabilities", *J. Comput. Phys.* 227, 6754-6778, 2008.
- <sup>13</sup>A. D. Pierce, *Acoustics: An introduction to its physical principles and applications*, Acoustical Society of America, 1991.